RADS RDSAR
Algorithm Theoretical Basis Document
Version 0.3

Remko Scharroo

1 August 2014

This document was typeset with LaTeX 2_ε.
The layout was designed by Remko Scharroo © 1993–2002

Contents

Chapter 1
Introduction

1.1 Purpose and scope

This document describes the theoretical background behind the creation of Pseudo Low Resolution Mode (Pseudo LRM or PLRM) waveform from CryoSat-2 Synthetic Aperture Radar (SAR) echoes. This conversion technique is also referred to as Reduced SAR (RDSAR).

CryoSat-2 operates in three different modes: LRM, SAR, and SARin (SAR interferometric mode). The operating modes are switched at the edges of a predetermine mode mask (Figure 1.1) such that it will operate in a given mode in a given geographical area. The mode mask is regularly updated to include the changing of ice sheets. Generally CryoSat-2 is operating in LRM mode over most of the oceans, SAR over some coastal areas and a few selected boxes in the open ocean, SARin over the edges of ice shelves and mountain glaciers.

LRM is the classical mode used my all historical radar altimeters, pulsing between 2000 and 4000 times per second. The pulse interval is large enough that the returned echoes are uncorrelated and no SAR technique can be applied. CryoSat-2 is the first radar altimeter to also provide a SAR mode, transmitting pulses at a much higher frequency (18 kHz) but only one third of the time, waiting two thirds of the time to receive the echoes (Figure 1.2).

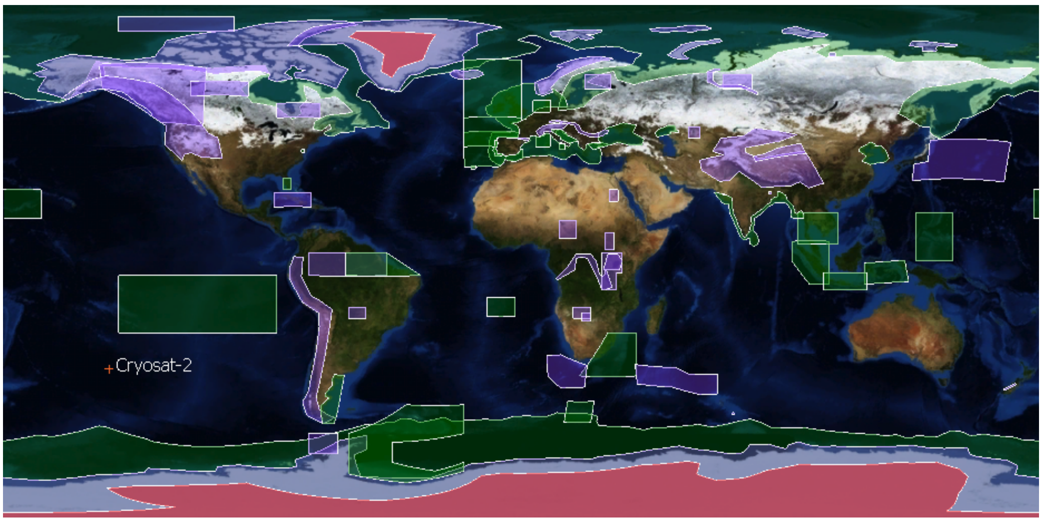

Figure 1.1 The current CryoSat-2 mode mask (version 3.4). Green is SAR mode, purple is SARin mode, other areas are in LRM mode.

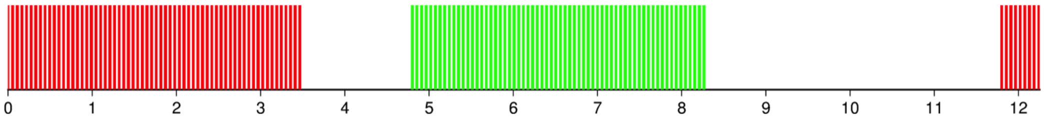

Figure 1.2 Illustration of one burst of pulses (red) and reception of their echoes (green). The total burst duration is 11.8 ms.

The processing of the SAR echoes is significantly different from the traditional LRM mode. In the first case the complex echoes are averaged coherently: their phase is taken into account when summing the complex echoes. In the second case the echoes are averaged incoherently: their phase is not taken into account when summing just the power of the echoes.

The intent of the RDSAR technique is to create waveforms that look like LRM mode waveforms, but are not that entirely because in SAR mode the instrument is not transmitting at a constant rate, but has this two-thirds waiting time mentioned before. Hence the name Pseudo LRM waveforms.

For the creation of the Pseudo-LRM waveforms we go back to the CryoSat-2 Level 1A product known as FBR (Full Bit Rate). That product holds all the echoes that were received in complex form. The result can be regarded a Level 1B product, similar to the standard CryoSat-2 Level 1B products.

The Pseudo-LRM data have been merged with LRM data and have been available via RADS since October 2012. Since then, NOAA has developed some other techniques to process the SAR data, taking advantage of the higher spatial resolution it can provide.

The processing of CryoSat-2 LRM and PLRM data by Altimetrics and NOAA within and outside of the framework of CP4O has been reported at various meetings and in various publications:

- CryoSat-2 Quality Working Group meetings: [*Scharroo et al.*, 2012a,b,c].
- Coastal Altimetry workshops: [*Scharroo et al.*, 2012d].
- Ocean Science Topography Science Team Meetings: [*Scharroo et al.*, 2012e].
- CryoSat-2 User workshops: [*Scharroo et al.*, 2013a].
- ESA Living Planet Symposia: [*Scharroo et al.*, 2013b].
- Other publications: [*Smith and Scharroo*, 2014].

1.2 Acronyms

ATBD	Algorithm Technical Basis Document
CAL2	Calibration mode 2
CP4O	CryoSat Plus for Oceans
ESA	European Space Agency
FAI	Fine range word
FBR	Full bit rate
FFT	Fast Fourier Transform
I/Q	In-phase (real) and Quadrature (imaginary)
IPFDB	Instrument Processing Facility Data Base
L1A	Level 1A
L1B	Level 1B
L2	Level 2
LAI	Coarse range word
LPF	Low-pass filter
LRM	Low Resolution Mode
PLRM	Pseudo Low Resolution Mode
RDSAR	Reduced Synthetic Aperture Radar
SAR	Synthetic Aperture Radar

Chapter 2

Algorithm description

2.1 Processing steps

The RDSAR technique comprises the following steps, starting with the L1A FBR product.

1. Gather 4 bursts of 64 echoes.
2. Adjust the FAI for each burst.
3. Align the echoes horizontally.
4. Align the echoes vertically (optional).
5. Correct echo amplitude and phase.
6. Zero pad the echoes.
7. Perform a 1-dimensional FFT, horizontally.
8. Incoherently average the individual waveforms.
9. Apply low-pass filter correction.
10. Rescale the waveform.

These steps are further described in detail in Section 2.2.

The result are 20-Hz waveforms similar to those found on the L1B LRM products. After that the PLRM data can be processed to L2 as if they were real LRM data (with some caveats).

Since the power of the waveforms is scaled such that the maximum value for any sample is always 65535, a detailed description of the power amplification is necessary. This is done in Section 2.4.

2.2 Algorithm definition PLRM waveforms

2.2.1 Gather 4 bursts of 64 echoes

During every 20-Hz radar cycle, CryoSat produces 4 bursts. Each burst lasts about 3.5 ms, in which 64 pulses are produced at a frequency of about 18 kHz. After a waiting period to receive the echoes, the next burst starts at 11.8 ms intervals (Figure 1.2.

The FBR data contain during each 20-Hz cycle, 4 sets of 64 echoes, each containing 128 complex (I and Q) samples. These echoes from the FBR are already deramped in the time domain but have not yet been calibrated. That means that their power is relative to the gain settings and the phase is determined by the location of the range window. But neither of these (gain nor range window delay) are calibrated for instrumental effects.

The 4 bursts are individually time tagged and geolocated on the FBR product. To produce the referencing of the final 20-Hz PLRM waveforms, the time in between the second and third burst is computed. The geolocation of the 20-Hz sub-satellite point and altitude is then computed by interpolating the satellite orbit. The FBR products always contain all four bursts per radar cycle, so there are no complexities when they are not all 4 available.

2.2.2 Adjust the FAI for each burst

The position of the waveform leading edge is kept close to the sample 34 (counting from 0 to 127) by the on-board tracker. The uncorrected window delay is given by the coarse range word (LAI), which has a digitisation of 4 range gates. In addition, the tracker gives an estimate of how far the waveform leading edge will be displaced from the optimal position, known as the fine range word (FAI) which has a range of -128 to 127 and is equivalent to ± 2 range gates.

The tracker is noisy, and has a tendency to misestimate the range rate. When the on-board tracker is producing a higher or lower rate than the actually rate of change of the range, the waveform will be blurred. Over oceans, the altitude rate is a better approximation of the range rate than the one suggested by the on-board tracker. Hence we will adjust the FAI estimates such that they will be in accordance with the altitude rate, while taking into account that the LAI may change between bursts.

Say that LAI (the uncorrected window delay in units of range), FAI (in units of range), and the orbital altitude h are arrays of four elements, one for each burst in a radar cycle. Then the array FAI is recomputed as follows:

$$\mathrm{FAI} = (\overline{\mathrm{LAI} + \mathrm{FAI} - h} + h - \mathrm{LAI}) \tag{2.1}$$

where the overline denotes the average over the four elements of the arrays.

2.2.3 Align the echoes horizontally

The complex power for each of the samples (bins) for each echo within a burst is given a phase shift equivalent to the change of range compared to the new 20-Hz time tag. Here we have to distinguish both the change of range between the bursts given by the adjusted FAI from the previous processing step and the change of range within a burst. In both cases the change of range is based on the altitude rate rather than the on-board tracker information. However, we do take here into account (in the adjusted FAI numbers) that the LAI may change between bursts.

The phase shift ϕ to be applied to sample k (running from 0 to 127) of echo p (running from 0 to 63) is the sum of three components:

$$\phi = (k - 63.5)\phi_k + \phi_d + \phi_c \tag{2.2}$$

where ϕ_k is the phase advance between samples, which in turn is determined by 2-way time delay, τ_{FAI} associated with the change in adjusted FAI (the change of range *between* the bursts) and the 2-way time delay associated with the change of range *within* a burst, τ.

$$\phi_k = (\tau_{\mathrm{FAI}} + \tau)\,\omega_k \tag{2.3}$$

where $\tau_{\rm FAI}$ is determined by the adjusted FAI, τ depends on the pulse number p, the altitude rate $\dot{h}$, the time between pulses (55 μs), and ω_k is the frequency change between samples:

$$\tau_{\rm FAI} = 2\,\mathrm{FAI}/c \tag{2.4}$$

$$\tau = (2p - 63)\tau_p \tag{2.5}$$

$$\tau_p = \dot{h}(55\mu\mathrm{s})/c \tag{2.6}$$

$$\omega_k = -2\pi/(400\mathrm{ns}) \tag{2.7}$$

2.2.4 Align the echoes vertically

An additional (but not essential) step in the echo alignment is the phase shift ϕ_d in equation (2.2). This shift is intended to align the echoes "vertically", meaning that after a 2-dimensional FFT the peak power will be in the nadir Doppler bin. This "Doppler shift" equals

$$\phi_d = 2\pi f \tau \tag{2.8}$$

where f is the radar frequency of 13.575 GHz. Figure 2.2 shows a single burst converted by a 2-dimensional FFT.

Because we will actually perform a 1-dimensional FFT, this step is not essential and has no impact on the final waveform obtained.

2.2.5 Correct the echo amplitude and phase

Because the altimeter power and phase is not entirely stable (constant) during a burst, each of the 64 pulses (echoes) within a burst needs their amplitude and phase corrected. The amplitude factors (increasing from the first pulse to the last, with an average of 1) and phase shifts (starting with a zero phase shift and increasing with increasing pulse number) are retrieved from the IPFDB file `CS_OPER_AUX_IPFDBA_20101111T101900_99999999T999999_0002.EEF`. The phase shift ϕ_c is one of the three components in equation (2.2).

2.2.6 Zero-pad the echoes

Zero-padding is a technique used to minimise the loss of information when performing the subsequent 1-dimensional FFT and incoherent averaging. This loss of information and its remedy was proposed by *Jensen* [1999] and was only proven to be actually beneficiary by *Smith and Scharroo* [2014] based on the processing of CryoSat-2 FBR data.

Zero-padding is obtained by adding 64 (complex) zeros on each side of the 128 bins of complex echoes. This is because the zero frequency is in the middle of the 128 bins, and negative and positive frequencies run the the left and right respectively. The extra 64 (complex) zeros does simply suggest zeroes at higher negative and positive frequencies.

2.2.7 Perform a 1-dimensional FFT, horizontally

Each of the 64 pulses in 4 bursts is now individually FFTed. This results in 256 very noisy "individual waveforms" of 256 complex samples each, as illustrated in the right column in Figure 2.1. Note that the "leading edge" of the each of these "waveforms" is properly aligned on the tracking gate (34).

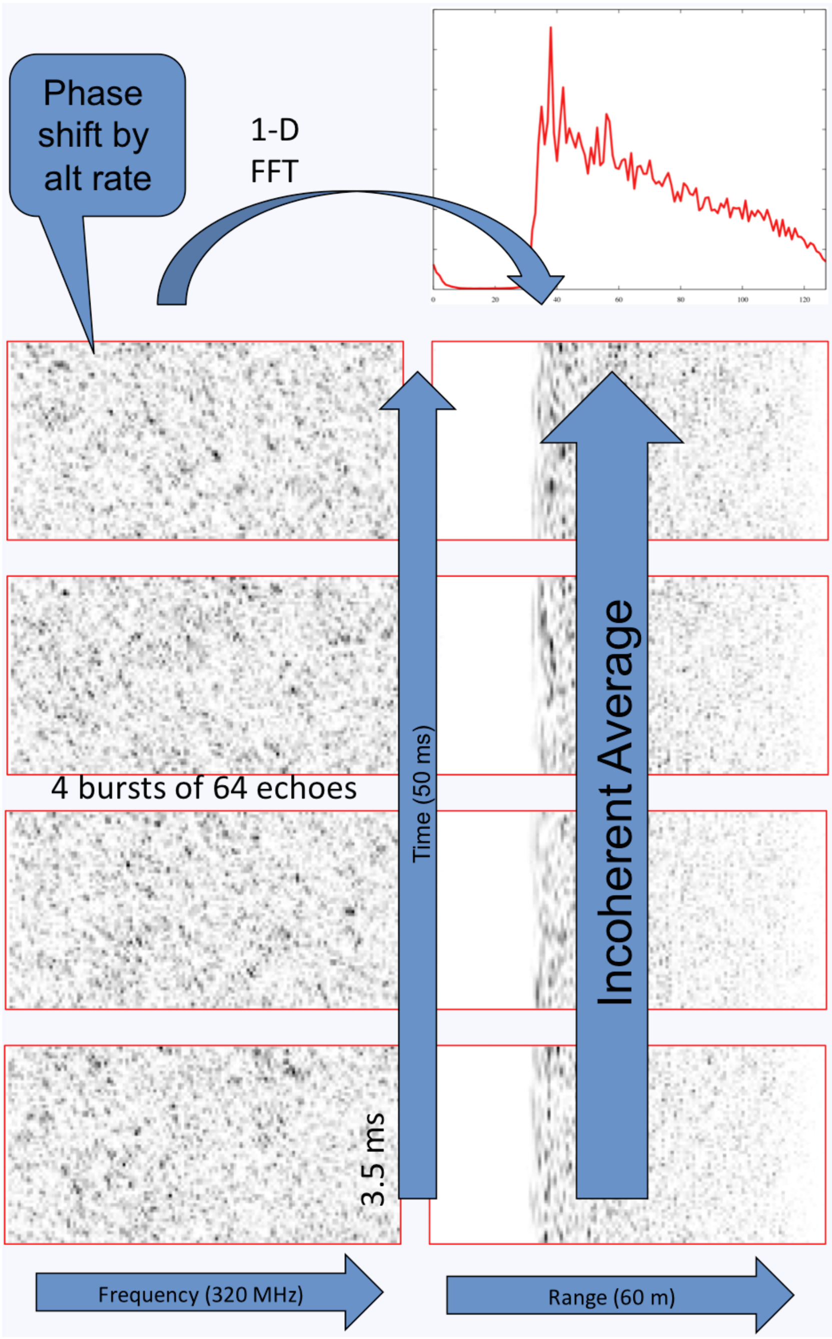

Figure 2.1 Four bursts of 64 complex echoes (left column) are phase shifted so that after 1-D FFT the individual waveforms are all aligned (right column). Those waveforms are then incoherently averaged to form a single 20-Hz PLRM waveform. Zero padding is not shown in the graph. Of the echoes and individual waveforms only the power is shown (black begin largest), not the phase, however each are built of complex numbers.

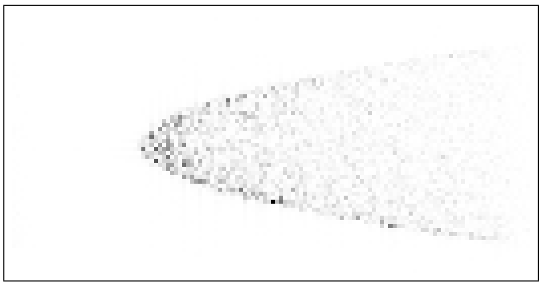

Figure 2.2 A single burst after 2-dimensional FFT. The peak power is aligned vertically such that it falls on the nadir Doppler bin.

2.2.8 Incoherently average the individual waveforms

The 256 ″individual waveforms″ are incoherently averaged (in fact, they are summed in our implementation). This means that each sample k of the resulting 20-Hz PLRM waveform is determined by summing the power across the 256 ″individual waveforms″:

$$W(k) = \sum_{p=0}^{255} \sqrt{I(p,k)^2 + Q(p,k)^2} \tag{2.9}$$

where $W(k)$ is the waveform power for each sample (k runs from 0 to 255) and $I(p,k)$ and $Q(p,k)$ are the complex numbers of the individual waveforms after FFT.

2.2.9 Apply low-pass filter correction

The individual samples of the resulting waveform need to be adjusted in power to correct for the effect of the low-pass filter (LPF) used to separate the deramped signal after differencing the received radar echoes with a duplicate of the transmitted pulse. Because this differencing also creates a signal with the frequencies summed, an LPF filter is used to extract only the lower (differenced) frequency.

However, the LPF filter has imperfections that result in a change in effective power from one sample to the next. This is characterised by the CAL2 calibration and the results are available in the IPFDB. Because the LPF correction appears to be constant, we use the values from IPFDB file `CS_OPER_AUX_IPFDBA_20101111T101900_99999999T999999_0002.EEF`.

In order to correct the 256 samples we have obtained after zero-padding, we expanded the LPF correction table from 128 to 256 samples by means of linear interpolation.

2.2.10 Rescale the waveform

The waveforms are rescaled such that the highest value for any sample in a waveform is always 65535. The way to compute the proper power from these waveforms is described in Section 2.4.

2.3 Range computation

The PLRM range measurement can be determined by adding the estimated epoch of the leading edge of the wave form (converted to units of range) to the tracker range. In other words:

$$\texttt{range\_20hz\_ku} = \texttt{range\_tracker\_20hz\_ku} + r \quad (2.10)$$

where

- range_20hz_ku is the total calibrated one-way range provided on the RADS PLRM products.
- range_tracker_20hz_ku is the tracker range relative to gate 34 (starting from 0), corrected for USO drift, Doppler correction and internal calibration, as given on the RADS PLRM products.
- r is the range correction determined by the tracker, giving the position of the leading edge relative to gate 34.

2.4 Power conversion

In the RADS PLRM data provided in the framework of CP4O, with each PLRM waveform a scale factor is provided. This scale factor is computed as follows:

$$G = -G_W - G_{\mathrm{TxRx}} - G_{\mathrm{S,SAR}} - G_{\mathrm{AGC}} - G_{\mathrm{Tx}} - G_N \quad (2.11)$$

where

- G is the waveform scale factor in dB; this is stored as variable waveform_scale_20hz on the PLRM product.
- G_W is the scale factor needed to normalise the PLRM waveforms as discussed in 2.2.10, expressed in dB.
- G_{TxRx} is the transmitter and receiver gain provided on the L1A product (in dB).
- $G_{\mathrm{S,SAR}}$ is the processor gain in SAR mode. Theoretically $G_{S,SAR}$ is 126.227 dB, but comparing LRM to PLRM leads to 125.8 dB, which value we have used.
- G_{AGC} is the AGC setting, properly corrected from integer values (in dB).
- G_{Tx} is the transmit power (in dBW).
- G_N is the nominal attenuation at nominal altitude (h_N = 735 km) and with zero off-nadir angle (G_N = –151.125 dB)

In order to compute the backscatter coefficient σ^0 from the waveform scale and other parameters, add the following components:

$$\sigma^0 = G + G_{\mathrm{amp}} + G_\eta + G_h + G_\xi + G_{\mathrm{SWH}} \quad (2.12)$$

where

- σ_0 is the backscatter coefficient; this is stored as variable sig0_20hz_ku on the RADS PLRM products.
- G is the waveform scale factor, expressed in dB, as defined in 2.11 above.
- G_{amp} is the amplitude determined by the retracker based on the waveforms normalised to have a peak value of 65535, converted to dB. This means that the values are generally around 48 dB ($= 10 \log_{10}(65535)$).

- G_η is an attenuation correction for the flattening of the Earth, then converted to dB.

$$G_\eta = 10 \log_{10} \left(\frac{1 + h/R}{1 + h_N/R} \right) \tag{2.13}$$

where h is the orbital altitude, h_N is the nominal altitude (735 km), R is the mean radius of the Earth (6371 km). The absolute value of this correction is generally smaller than 0.01 dB.

- G_h is the attenuation because of non-nominal altitude, converted to dB.

$$G_h = 30 \log_{10}(h/h_N) \tag{2.14}$$

- G_ξ is the attenuation because of off-nadir angle, ξ, expressed in dB.

$$G = \frac{40\xi^2}{\gamma \ln 10} \tag{2.15}$$

- G_{SWH} is the attenuation because of SWH, expressed dB. This is, however, so small (order 0.001 dB) that it can be handily ignored.
- γ is an antenna aperture parameter based on the full beam width β of the antenna, such that

$$\gamma = \frac{2}{\ln 2} \sin^2 \frac{\beta}{2} \tag{2.16}$$

- β is the (weighted) beam width of the elliptical CryoSat-2 antenna, whose square is determined by the harmonic mean of the square of the along-track and cross-track beam widths (1.10° and 1.22°, respectively).

$$\beta^2 = \frac{2}{1/\beta_1^2 + 1/\beta_2^2} \tag{2.17}$$

Bibliography

Jensen, J. R. (1999), Radar altimeter gate tracking: Theory and extension, *IEEE Trans. Geosci. Rem. Sens.*, *37*(2), 651–658.

Scharroo, R., W. H. F. Smith, and M. C. Naeije (2012a), Validation of CryoSat test data set over open oceans (LRM and FDM, Level 1 and 2), *Tech. rep.*, Altimetrics LLC.

Scharroo, R., W. H. F. Smith, and M. C. Naeije (2012b), Updated validation of CryoSat test data set over open oceans (LRM and FDM, Level 1 and 2), *Tech. rep.*, Altimetrics LLC.

Scharroo, R., W. H. F. Smith, and M. C. Naeije (2012c), Re-updated validation of CryoSat test data set over open oceans (LRM and FDM, Level 1 and 2), *Tech. rep.*, Altimetrics LLC.

Scharroo, R., W. H. F. Smith, J. L. Lillibridge, and E. W. Leuliette (2012d), Calibration and validation of combined conventional and reduced SAR mode data over oceans and in the coastal regime, presented at Sixth Coastal Altimetry Workshop, Riva del Garda, Italy, 20-21 September 2012.

Scharroo, R., W. H. F. Smith, J. L. Lillibridge, and E. W. Leuliette (2012e), Global Cal/Val of CryoSat-2 LRM and SAR data over oceans, Ocean Science Topography Science Team Meeting, Venice, Italy, 27-29 September 2012.

Scharroo, R., W. H. F. Smith, E. W. Leuliette, and J. L. Lillibridge (2013a), The performance of CryoSat-2 as an ocean altimeter, in *Proc. of the CryoSat-2 Third User Workshop, Dresden, 12-14 March 2013, Eur. Space Agency Spec. Publ., ESA SP-717*, p. 5 pp.

Scharroo, R., W. H. F. Smith, E. W. Leuliette, and J. L. Lillibridge (2013b), CryoSat-2: The other ocean altimeter, ESA Living Planet Symposium, Edinburgh, Scotland, 9-13 September 2014.

Smith, W. H. F., and R. Scharroo (2014), Waveform aliasing in satellite radar altimetry, *IEEE Trans. Geosci. Rem. Sens.*, doi:10.1109/TGRS.2014.2331193, in press.